
Hindrance in Super heavy elements formation by fission dynamics studies

K. Kalita^{1*}, G. Narzary^{1,2}, M. Bhuyan², A. Sen³, T. K. Ghosh³, L. Sharma¹

¹*Department of Physics, Gauhati University, Guwahati -781014, India*

²*Department of Physics, Rangia College, Rangia-781354, India*

³*Variable Energy Cyclotron Centre (VECC), 1/AF, Bidhan Nagar, Kolkata-700064, India*

Email: kkalita@gauhati.ac.in

Abstract :

Fission dynamics studies induced by heavy ions are carried out around and well above the fission barrier to know about the role of compound fission and non-compound fission events. The behaviour of fission dynamics at low and above the energies is quite different in terms of mean field interaction and non-mean field interactions. It seems that the contributions from non-compound fission and break-up-related incomplete fusion are the main observables in the experiment, but separating them is quite challenging. These phenomena are hindering the formation of super-heavy nuclei in most cases of heavy ion reactions.

Key words : Fusion-fission, Quasi-fission, NCN.

*A part of the MS was presented by the first author as an invited speaker at the NaSAEAST-25 held at Gauhati University during December 26-27, 2025.

1. Introduction:

The systematic study of fusion-fission dynamics is essential for understanding the complex evolution of composite nuclear systems formed in heavy-ion reactions, especially at energies near the Coulomb barrier. This energy regime is particularly important for the synthesis of superheavy elements, where the excitation energy must lie just above the fusion threshold to maximize the formation and survival probability of heavy evaporation residues [Bjørnholm et al.,1982; Blocki et al., 1986].

However, experimental evidence shows that complete fusion is not always achieved. A significant fraction of reaction trajectories is diverted by the competing processes, which hinder fusion. These include not only fission of the fully equilibrated compound nucleus (CN), but also non-compound nucleus (NCN) mechanisms such as fast fission [Borderie et al., 1981; Ngô et al., 1986; Lebrun et al., 1979], pre-equilibrium fission [Ramamurthy and Kapoor 1985], and quasi-fission (QF) [Back., 1985. Tōke et al., 1985]. These processes compete with evaporation residue formation and depend strongly on parameters such as excitation energy and angular momentum.

In compound nucleus fission, the system reaches full equilibration in all degrees of freedom before evolving toward fission through a mass-symmetric configuration at the unconditional saddle point of the potential energy surface. In contrast, QF occurs when the interacting dinuclear system fails to achieve complete equilibration and instead evolves toward fission through a mass-asymmetric configuration corresponding to a conditional saddle point [Nasirov et al., 2013; Möller & Sierk 2003, Diaz-Torres , 2006; Swiatecki., 1981]. This distinction arises due to incomplete equilibration in mass and shape degrees of freedom in the QF process.

The entrance channel properties of the reacting nuclei play a critical role in governing the reaction dynamics and the onset of QF. Key parameters include the product of the projectile and target charges ($ZP ZT$), mass asymmetry relative to the Businaro-Gallone critical value, shell effects, nuclear deformation, compound nucleus fissility, and neutron-to-proton ratio [Swiatecki ,1981; Prasad et al., 2010; Shamlath et al., 2016; Hinde et al., 1995; Prasad et al., 2015 ; Nishio et al., 2015; Hinde et al ,1996]. Over the years, these factors have significantly contributed to both experimental and theoretical understanding of heavy-ion-induced reactions.

To disentangle compound nucleus fission from competing NCN processes, several experimental observables have been widely employed. These include the measurement of fission fragment mass distributions and their widths [Prasad et al., 2010; Shamlath et al., 2016; Kavita et al., 2019; Reddy et al., 2024], mass-angle correlations, angular anisotropies [Banerjee et al, 2016], evaporation residue cross sections [Hajara et al, 2022], and neutron multiplicities [Golda et al, 2013; Sharma et al., 2023]. Each of these observables provides complementary insights into the reaction mechanism and helps in identifying signatures of QF.

Numerous experimental investigations have examined systems leading to the same compound nucleus but formed through different entrance channels. In several cases, an observed broadening in the fission fragment mass distribution has been attributed to QF. However, other studies have shown that the data can be explained within the framework of statistical models, suggesting the dominance of compound nucleus fission and highlighting inconsistencies in the interpretation of experimental results [Chaudhuri et al., 2015].

Similarly, measurements of evaporation residue cross sections and angular distributions have produced mixed conclusions. While some reactions exhibit suppression of evaporation residues, indicative of NCN contributions [Hajara et al., 2022], others are well described by statistical saddle-point models, implying negligible QF effects [Chaudhuri et al., (2015)] Investigations into shell effects have also yielded contrasting results, with some studies reporting no significant influence on mass distributions, while others observe clear signatures through anisotropy and neutron emission measurements [Golda et al., 2013].

In the present study, the fission fragment mass distribution of the compound nucleus ^{206}Po , formed through the $^{30}\text{Si} + ^{176}\text{Yb}$ reaction, has been investigated at energies in the vicinity of the Coulomb barrier. The primary objective is to examine the role of entrance channel mass asymmetry and nuclear deformation in governing fission dynamics. The continued observation of asymmetric mass division in low-energy fission, despite the expectations of the liquid drop model [Bohr and Wheeler, 1939; Meitner, 1950] and supported by surprising results in lighter systems such as mercury and sub-lead nuclei [Prasad et al., 2015; Nishio et al., 2015 ; Andreyev et al., 2010], remains a key motivation for such investigations.

In addition to this, the reaction $^{16}\text{O} + ^{205}\text{Tl}$ has been studied at significantly higher beam energies ranging from 330 MeV to 363 MeV, leading to the formation of the compound nucleus ^{221}Ac . This higher energy regime is particularly useful for probing the contribution of NCN processes and understanding their role in suppressing compound nucleus formation. Such studies provide valuable insight into the competition between fusion and alternative reaction pathways.

The key characteristics of the reaction systems under investigation are summarized separately, and detailed descriptions of the experimental setup, results and discussion, and conclusions are presented in the following sections.

2. Experimental Setup:

The experiments were carried out at two accelerator facilities in India to investigate fission fragment characteristics under different reaction conditions. One set of measurements was performed at the Inter University Accelerator Centre (IUAC), New Delhi using the 15-UD Pelletron accelerator. A pulsed beam of silicon nuclei (^{30}Si), with a pulse separation of 250 ns and a pulse width of approximately 1 ns, was delivered in the laboratory energy range of 124 -137 MeV. The beam was incident on a ^{176}Yb target of thickness about $130 \mu\text{g}/\text{cm}^2$, prepared with a thin carbon backing ($\sim 25 \mu\text{g}/\text{cm}^2$). The target foil was mounted perpendicular to the beam direction at the center of the scattering chamber.

Fission fragments were detected in coincidence using two multiwire proportional counters (MWPCs), each having an active area of $20 \times 10 \text{ cm}^2$, mounted on movable arms inside the chamber as shown in Figure 1. The detectors were positioned symmetrically at $\pm 70^\circ$ with respect to the beam axis, corresponding to 90° in the center-of-mass frame, based on reaction kinematics. The distance between the target and each detector was maintained at 33 cm and 35 cm respectively. For beam monitoring and alignment, two silicon surface barrier detectors were placed at $\pm 20^\circ$. The MWPCs, operated with low-pressure isobutane gas ($\sim 4 \text{ mbar}$), provided high-resolution timing and position information, with spatial resolution better than 1.5 mm achieved through delay-line readout. Time-of-flight (TOF) and position signals were recorded in list mode using a ROOT-based data acquisition system.

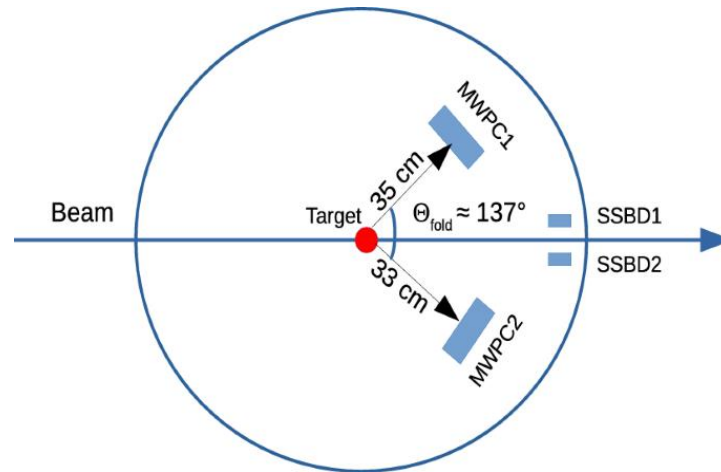


Figure 1: A typical Schematic diagram of the experimental setup in Fission Expt.

The second set of measurements was carried out at the Variable Energy Cyclotron Centre(VECC), Kolkata using the K-500 superconducting cyclotron. In this case, an oxygen beam (^{16}O) with energies of 330 MeV and 363 MeV was directed onto a ^{205}Tl target thickness of approximately $300 \mu\text{g}/\text{cm}^2$. The target was mounted at an angle of 120° relative to the beam axis. Figure 2 is the internal view of the experimental setup where the detection of the resulting fission fragments was accomplished using two position-sensitive MWPCs of active area $20 \times 6 \text{ cm}^2$ placed within the scattering chamber. One detector was located at 80° and a distance of 22.5 cm from the target, while the other was positioned at 60° and 24.2 cm.

Both detectors were operated with isobutane gas at a pressure of about 3 Torr, ensuring that quasi-elastic and low-mass deep-inelastic products passed through without significant interaction. The experimental setup enabled the simultaneous measurement of position, energy loss, and time-of-flight of coincident binary fragments. Data acquisition in this case was performed using the LAMPS software, allowing comprehensive event-by-event recording of fragment properties. Together, these complementary setups provided high-resolution measurements of fission fragment observables under varied entrance channel conditions, enabling a detailed investigation of the underlying the reaction dynamics.

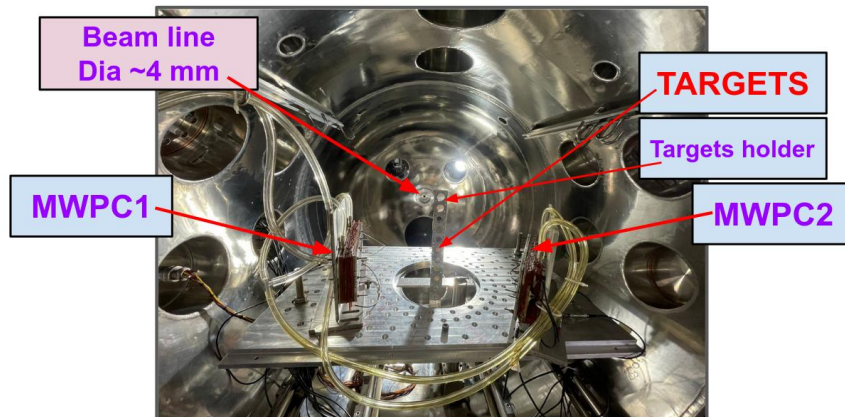


Figure 2: Internal view of the experimental setup, illustrating the beamline, target assembly, target holder, and the arrangement of the two multi-wire proportional counter (MWPC) detectors.

3. Results & Discussion:

The identification of fission events was achieved by distinguishing them from elastic scattering through the timing correlation between signals recorded in the two MWPC detectors. A suitable gate was applied on this correlation, as illustrated in Figure 3, to isolate the desired events. The list-mode data acquired from the detectors contained information on the time of flight (TOF) as well as the X and Y position coordinates of the detected fragments.

For data analysis, all time-to-digital converters (TDCs) were carefully calibrated using an ORTEC time calibrator, which provides pulses at well-defined time intervals. Position calibration was carried out based on the known active area of the detectors. Using the calibrated position data and the experimental geometry, the fragment trajectories were transformed into spherical polar coordinates, namely the laboratory angles θ ($\theta_{1,\text{lab}}$, $\theta_{2,\text{lab}}$) and φ ($\varphi_{1,\text{lab}}$, $\varphi_{2,\text{lab}}$), for the two coincident fission fragments.

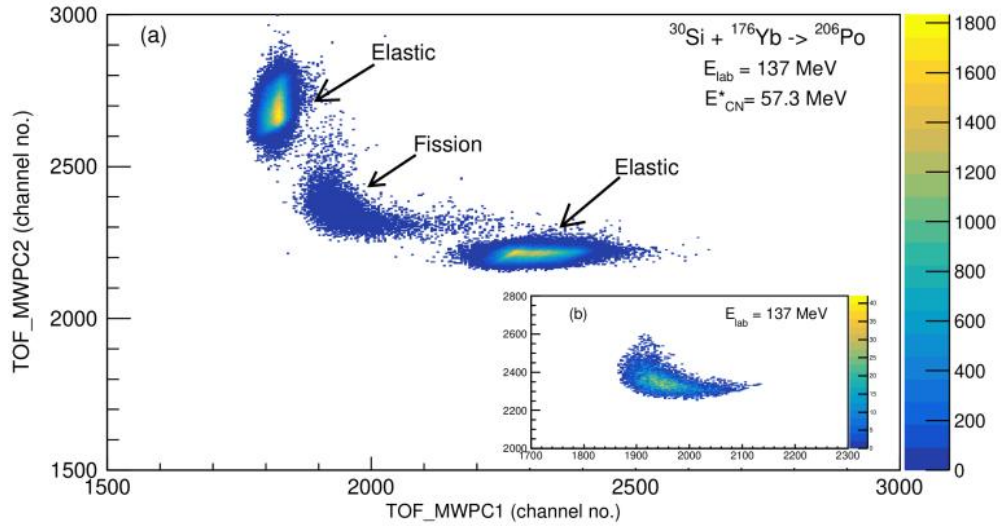


Figure 3: Plot of time-of-flight (TOF) spectra for the $^{30}\text{Si} + ^{176}\text{Yb}$ reaction at $E_{\text{lab}} = 137 \text{ MeV}$ of the two MWPCs at IUAC, New Delhi. (a) The spectra of all collected events (elastic and fission). (b) Gated fission events.

The folding angle distribution of the fragments was then constructed, and its peak positions were found to be in good agreement with the expected values corresponding to full momentum transfer between the projectile and target. The correlation between folding angle and azimuthal angle for the detected fragments, as shown in the left panels of Figure 4, spans energies both below and above the Coulomb barrier.

To ensure the purity of the selected events and to eliminate contributions from background or incomplete momentum transfer processes, a gate was applied around the most intense region of the correlation spectrum, corresponding to the theoretically predicted values. Only the events within this gated region were used for further analysis, including the reconstruction of the fission fragment velocities.

The fission fragment mass distributions for the $^{30}\text{Si} + ^{176}\text{Yb}$ reaction at different excitation energies are shown in the right panels of Figure 4. These distributions display an overall symmetric shape, centered around a $0.5A_{\text{CN}}$ (i.e., half of the compound nucleus mass), and can be well described by a

single Gaussian function. The quality of the fits, indicated by the corresponding (χ^2) values, demonstrates good agreement between the experimental data and the Gaussian representation. This observation aligns with previous findings for the fission of $^{206,210}\text{Po}$ [Chaudhuri et al.,2015] and nearby compound systems [Shamlath et al.,2016] at excitation energies above approximately 40 MeV.

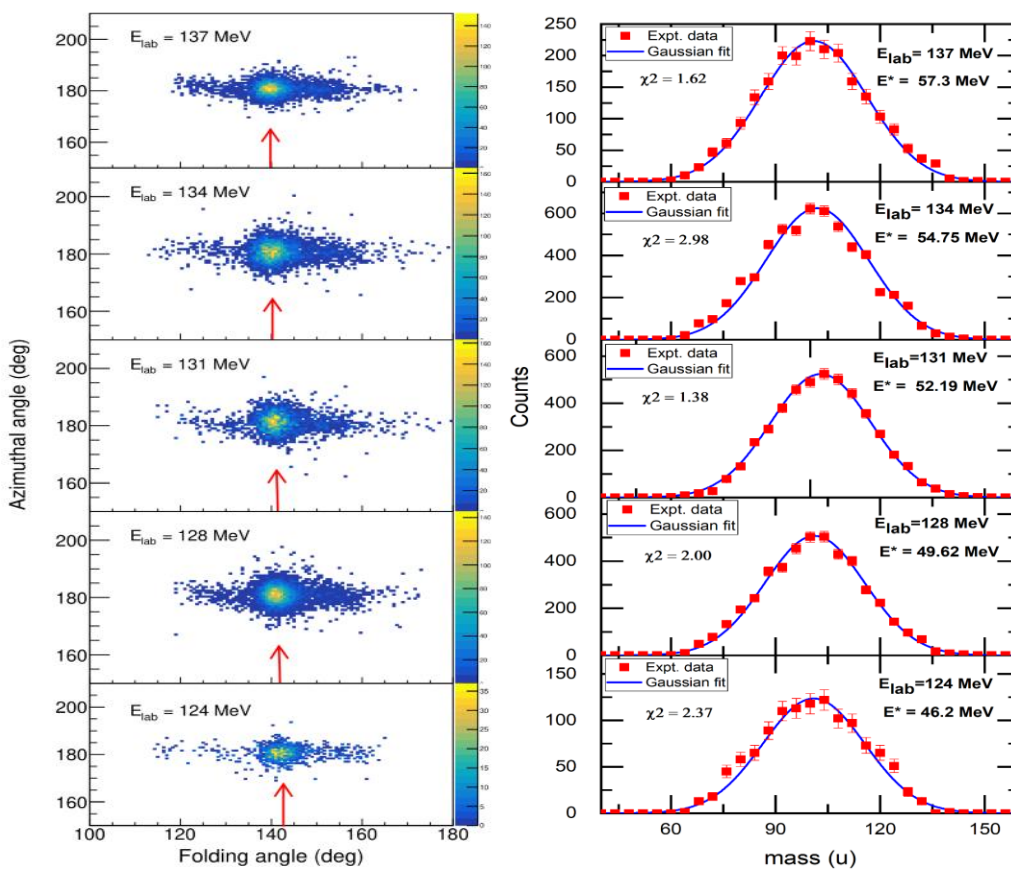


Figure 4: Left Panels: Distribution of polar (θ) and azimuthal (ϕ) angles of the fission fragments at different energies for the reaction $^{30}\text{Si} + ^{176}\text{Yb}$. The red arrow corresponds to the calculated folding angle from reaction kinematics. Right Panels: Fission fragments mass distribution at different excitation energies for the same reaction with single fit Gaussian function (blue solid line).

To further investigate the dependence of mass distribution on excitation energy, the width of the distribution (σ_m) was extracted from the standard deviation of the fitted Gaussian. Since the focus of the

present work is on the influence of entrance channel mass asymmetry and nuclear deformation, the (σ_m) values obtained from single Gaussian fits are considered, following established approaches in the literature [Andreyev et al.,2010; Vikas et al., 2024; Gupta et al., 2019]. The variation of (σ_m) with excitation energy for the $^{30}\text{Si} + ^{176}\text{Yb}$ and $^{12}\text{C} + ^{194}\text{Pt}$ systems, both leading to the same compound nucleus ^{206}Po but differing in entrance channel properties is shown in Figure 5. While (σ_m) increases with excitation energy for both systems, its magnitude is consistently larger for the more symmetric reaction compared to the asymmetric one at similar excitation energies.

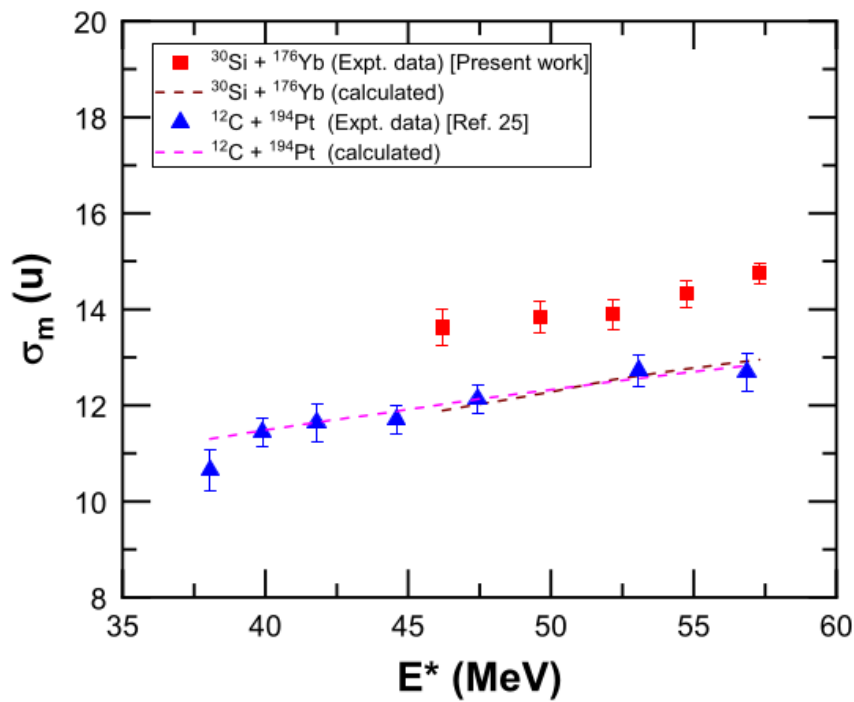


Figure 5: Dependence of variation of the mass width (σ_m) of the symmetric mass distribution as a function of excitation energy E^* for two different entrance channels forming ^{206}Po . The dashed line is for the calculated (σ_m) values.

Up to this point, we have observed that at lower energy ranges, complete momentum transfer occurs, resulting in a symmetric mass distribution, as shown in Figure 4. The larger values of (σ_m) compared to the Statistical Saddle-Point Model (SSPM) calculations, indicate that QF plays a significant role in

the reaction. However, the question arises: what happens at much higher beam energies, such as 330 MeV and 363 MeV?

To explore the reaction dynamics at very high beam energies and the formation of binary fission-like fragments in the $^{16}\text{O} + ^{205}\text{Tl}$ system, the folding angle correlation was analyzed, as depicted in Figure 6. The expected position of the folding angle peak, which corresponds to complete linear momentum transfer, was calculated using Viola systematic [Viola et al.,1985] and is marked with a pink vertical line within the black circular indicator. The folding angle distribution is shown in Figure 7, where a clear deviation from the predicted angle is observed. This shift suggests the involvement of NCN processes, such as QF or transfer-induced fission, which are more likely to occur at higher excitation energies due to shorter interaction times and incomplete equilibration. The distribution in Figure 7 reveals the presence of both complete and incomplete momentum transfer events, highlighting the competing mechanisms at play in this system.

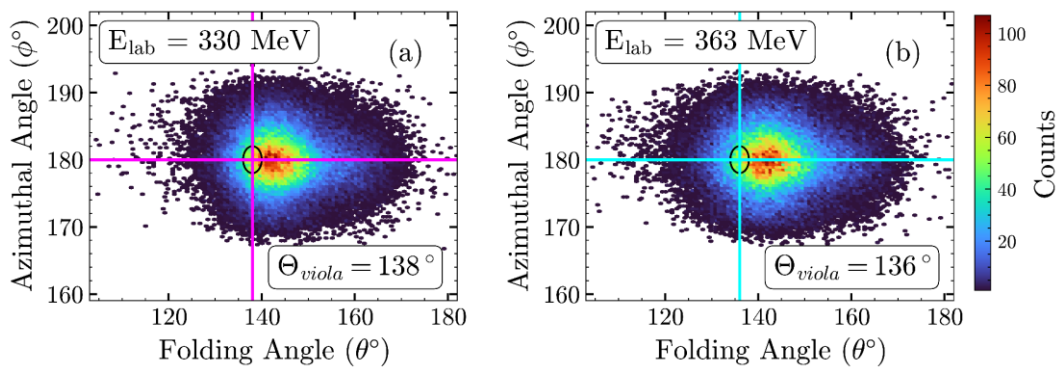


Figure 6: The angular correlation of the fragments produced in the reaction $^{16}\text{O}+^{205}\text{Tl}$ at energy $E_{\text{lab}}=330$ and 363 MeV. The vertical line marks full momentum transfer events around the folding angle predicted by the Viola systematic (Viola, et. al., 1985).

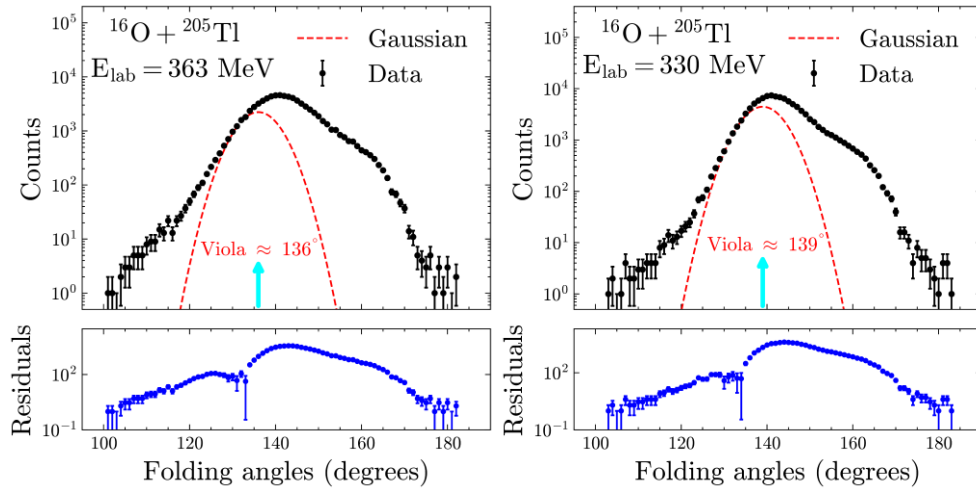


Figure 7: Folding angle distributions for the reaction $^{16}\text{O}+^{205}\text{Tl}$ at incident energies of 330 MeV and 363 MeV respectively. The corresponding residual plots are included to highlight deviations that may indicate contributions from NCN processes.

To quantify the contributions from NCN processes, the width of the folding angle distribution was compared to a reference width obtained from literature, where only compound nuclear fission was observed [Atreya, et al., 2024]. Since the folding angle is influenced by the reaction kinematics, this reference width was calculated by determining the angular coverage of the detectors and matching it with the experimental setup used in the present study. The residuals, displayed in the lower panels of Figure 7, reveal a distinct peak to the right of the Viola-predicted angle, which indicates a substantial contribution from NCN processes. A quantitative analysis shows that the area under the Viola-based compound fission region represents approximately 46% of the total, while the NCN contribution accounts for roughly 54% at 330 MeV. At 363 MeV, the NCN contribution increases to 68%.

To further validate and differentiate the contributions from complete compound fission and NCN processes, a gating procedure was applied around the Viola-predicted angle in the angular correlation. The mass distribution for the $^{16}\text{O} + ^{205}\text{Tl}$ reaction, forming the compound nucleus ^{221}Ac at 330 and 363 MeV beam energies, was then extracted, as shown in Figure 8. In the mass distribution, we observed a symmetric distribution, with a peak around half of the compound nucleus mass, as expected. When a single Gaussian function was fitted to the data, it closely matched the experimental results. This

confirms that the observed mass distribution is consistent with compound nucleus fission and exhibits the characteristic symmetric mass distribution.

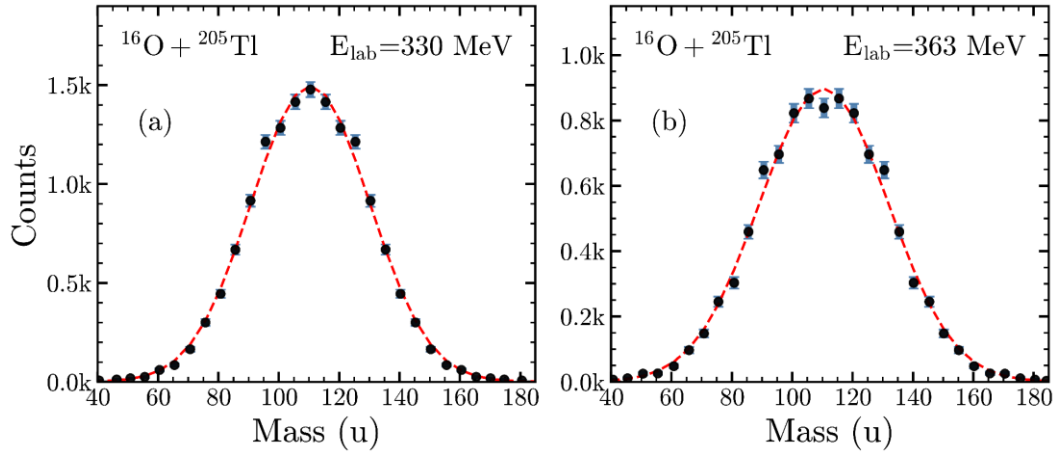


Figure 8: Mass distributions for the reaction $^{16}\text{O} + ^{205}\text{Tl}$ at incident energies of 330 MeV and 363 MeV, along with the corresponding residual plots.

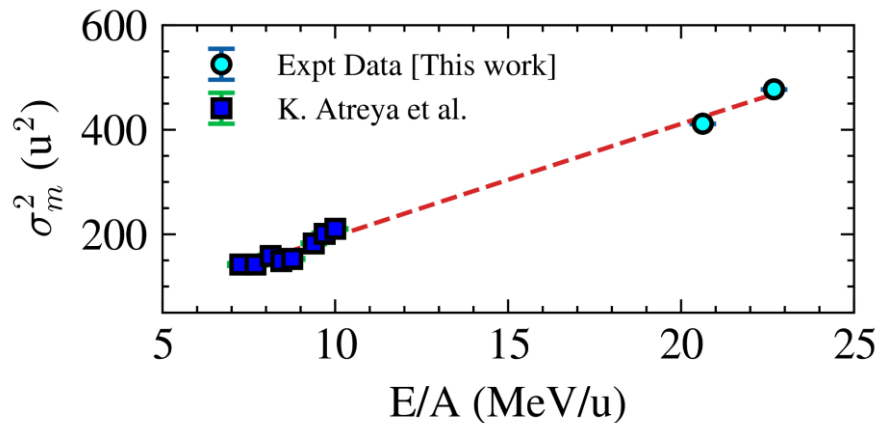


Figure 9: Variation of the measured standard deviation σ_m^2 (u^2) of the mass distributions with energy per nucleon (E/A) (MeV/u).

Figure 9 shows the variation of the measured standard deviation σ_m^2 (u^2) of the mass distributions as a function of energy per nucleon (E/A) in MeV/u . It is evident from the plot that the width of the mass distributions increases as the beam energy rises. When the data from lower energies, indicated by the

blue square markers, were fitted using a polynomial fit and compared with existing data from the literature [Atreya, et al., 2024], the results are consistent, both showing a clear increasing trend.

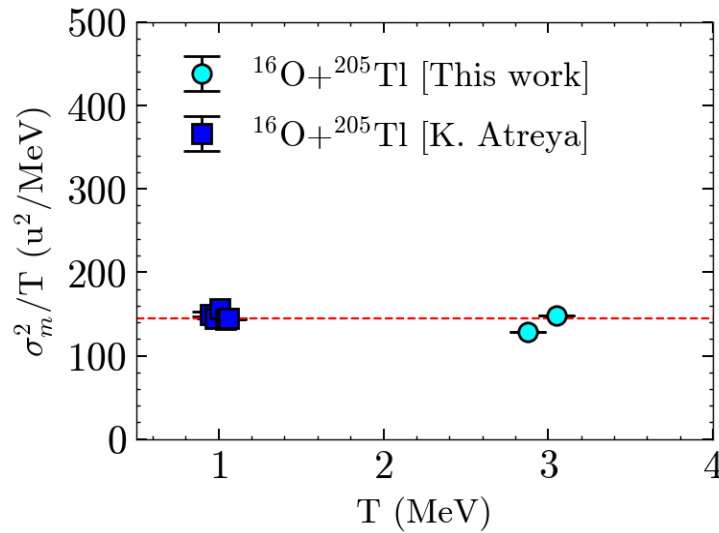


Figure 10: The width of the gated fission fragment mass distribution scaled with the temperature of the fissioning nucleus. Consistent with higher excitation energy and temperature effects.

In Figure 10, the width of the fission fragment mass distributions is presented and compared to the mass distributions of the same reaction at lower excitation energies [Atreya, et al., 2024]. It was found that the width of the mass distributions increases with temperature, following a trend where σ_m^2/T is constant for the data at 330 and 363 MeV beam energies. This suggests that the events are primarily the result of compound nuclear decay.

4. Conclusions:

In this study, we examined the fission fragment mass distribution for the $^{30}\text{Si} + ^{176}\text{Yb}$ reaction, forming the compound nucleus ^{206}Po , at lower excitation energies. The mass distribution width σ_m was fitted to a Gaussian function, and a higher magnitude of σ_m compared to statistical model calculations indicated quasi-fission (QF) processes, especially for symmetric entrance channel mass asymmetries. At higher



excitation energies (above 10 MeV/A), complete fusion is suppressed, necessitating modifications to the traditional Viola systematics. The width of the fission fragment mass distribution increases with excitation energy in both lower and higher energy ranges, indicating a dynamic fission process. At beam energies like 330 MeV and 363 MeV, the formation of superheavy elements (SHEs) is significantly suppressed, underlining the challenges in SHE synthesis. These results highlight the importance of considering factors like mass asymmetry, nuclear deformation, and entrance channel parameters in fission models. Further exploration of the single-particle shell model at lower excitation energies and sub-barrier regions, especially for ^{206}Po and nearby pre-actinide nuclei, could provide further insights into fission dynamics and SHE formation.

In summary, our analysis across a range of excitation energies has provided valuable insights into the interplay between compound nucleus fission and NCN processes, emphasizing the complex factors influencing fission dynamics and SHE synthesis.

Acknowledgements

The authors thank the accelerator staff of both IUAC, New Delhi & K-500 Superconducting Cyclotron, VECC Kolkata for providing high-quality heavy-ion beams and their technical support during the experiment. One of the authors (G.Narzary) also thanks the UGC-DAE CSR, Kolkata.



References:

- Andreyev, A. N., J. Elseviers, M. Huyse, P. Van Duppen, S. Antalic, A. Barzakh, T. E. Cocolios, V. F. Comas, *et al.*, (2010) New Type of Asymmetric Fission in Proton-Rich Nuclei, *Phys. Rev. Lett.* 105, 252502.
- Atreya, K., A. Sen, D. Paul, T. K. Ghosh, Kavita Rani, Md Moin Shaikh, K. Banerjee, C. Bhattacharya, Samir Kundu *et al.*, (2024) Fragment-mass distributions -induced reactions at energies well above the Coulomb barrier, *Phys. Rev. C* 109, 064620
- Back, B.B. (1985), Complete fusion and quasifission in reactions between heavy ions *Phys.Rev.C* 31 2104-2112,
- Banerjee, Tathagata, A. Jhingan, S. Nath, Gurpeet Kaur, R. Dubey, Abhushik Yadav, P. V. Laveen, A. Shamlath, M. Shareef *et al.* (2016), Fission fragment angular distributions in pre-actinide nuclei. *Phys. Rev. C* 34 044607
- Bjørnholm, S and W.J. Swiatecki (1982), Dynamical aspects of nucleus-nucleus collisions. *Nuclear Physics A* 391, 2, 27, 471-504
- Blocki, J.P., H. Feldmeier, W.J. Swiatecki (1986), *Nuclear Physics A*, 459, 1, 27 Pages 145-172
- Bohr, N. & Wheeler, J. A. (1939), The mechanism of fission. *Phys. Rev.* 56, 426–450
- Borderie, B., M. Berlinger, D. Gardès, F. Hanappe, L. Nowicki, J. Péter, B. Tamain, S. Agarwal, J. Girard, C. Grégoire, J. Matuszek & C. Ngô (1981), A possible mechanism in heavy ion induced reactions: “Fast fission process” *Z Physik A* 299, 263–271, <https://doi.org/10.1007/BF01443944>
- Chaudhuri, A., K. Ghosh, K. Banerjee, S. Bhattacharya, Jhila Sadhukhan, S. Kundu, C. Bhattacharya, J. K. Meena, G. Mukherjee *et al.*, (2024), No influence of a N=128 neutron-Shell closure in fission-fragment mass distribution *Phys. Rev. C* 92, 041601(R)
- Diaz-Torres, A., (2006), Competition between fusion and quasifission in a heavy fusing system: Diffusion of nuclear shapes through a dynamical collective potential energy landscape, *Phys. Rev. C* 74, 064601
- Golda, K.S., A. Saxena, V.K. Mittal, K. Mahata, P. Sugathan, A. Jhingan, V. Singh *et al.*, (2013) Determination of shell correction energies at saddle point using pre-scission neutron multiplicities *Nuclear Physics A*, 913, 2, 157-169.
- Gupta, Shilpi, C. Schmitt, K. Mahata, A. Shrivastava, P. Sugathan, A. Jhingan, K. S. Golda, N. Saneesh, M. Kumar, *et al.* (2019) Asymmetric fission around lead: The case of 198 Po, *Phys. Rev. C* 100, 0646008.

Hajara, K., Musthafa Musthafa, Midhun ,C. V., Shaima Akbar, (2022) Evaporation residue cross section measurements for the Si 30 + Yb 176 reaction, *Physical Review C* 105(4) DOI:10.1103/PhysRevC.105.044619.

Hinde, D. J., M. Dasgupta, J.R. Leigh, J.P. Lestone, J.C. Mein, C.R. Morton, J.O. Newton, H. Timmers (1995), Fusion-fission versus quasifission: Effect of nuclear orientation, *Phys Rev Lett.* 1995 Feb 20;74(8):1295- 1298. doi: 10.1103/PhysRevLett.74.1295.

Hinde, D J., M. Dasgupta, J.R. Leigh, J.C. Mein, C.R. Morton, J.O Newton, H. Timmers (1996). Conclusive evidence for the influence of nuclear orientation on quasifission *Phys Rev C Nucl Phys.* Mar;53(3):1290-1300. doi: 10.1103/physrevc.53.1290.

Kavita , K.S. Golda, T.K. Ghosh, A. Jhingan, P. Sugathan *et al.*, (2019), Fusion-fission dynamics of Pt188, 190 through fission fragment mass distribution measurements *Phys.Rev.C* 100 (2019) 2, 024626 DOI: 10.1103/PhysRevC.100.024626

Lebrun, C. F., Hanappe , J.F. LeColley , F. Lefebvres , C. Ngô, J. Péter, B. Tamain, (1979), Influence of angular momentum on the mass distribution width of heavy ion induced fission: What is the frontier between fission and quasi-fission? *Nuclear Physics A*, **321, 1**, 28 May 1979, 207-212.

Meitner, L (1950) Fission and nuclear shell model, *Nature* (London)165, 561 .

Möller, Peter & Arnold J. Sierk (2003), Why are new elements difficult to make? Fusion of two nuclei to produce heavy elements seems to be hindered by a competing process of 'quasi-fission'. New work builds a more complete picture, *Nature*, 422, 485–486.

Nasirov, A., Kim, K., Mandaglio, G., Giardina G., Muminov A., and Kim Y., (2013), Main restrictions in the synthesis of new superheavy elements: Quasifission and/or fusion fission. *Eur. Phys. J.A* **49**, 147 , <https://doi.org/10.1140/epja/i2013-13147-y>

Ngo, C., (SPhN, DAPNIA, Saclay) (1986) Fusion dynamics in heavy ion collisions *Prog.Part.Nucl.Phys.* 16 ,139-194 DOI: 10.1016/0146-6410(86)90004-9

Nishio, K., A.N. Andreyev , R. Chapman, X. Derkx, Ch.E. Düllmann, L. Ghys .F.P. Heßberger, K. Hirose, H. Ikezoe, J. Khuyagbaatar, B. Kindler , B. Lommel, H. Makii, I. Nishinaka , T. Ohtsuki , S.D. Pain, R. Sagaidak, I. Tsekhanovich , M. Venhart, Y. Wakabayashi , S. Yan, (2015), Excitation energy dependence of fragment-mass distributions from fission of 180,190Hg formed in fusion reactions of 36Ar + 144,154 Sm, *Physics Letters B*, 748, 89-94.

Prasad, E., D. J. Hinder, K. Ramachndran, E.Willium , M. Dasgupta, L.P. Carter, K .J .Cook , D. Y. Jeung, D. H .Luong *et al* ,(2015), *Phys.Rev C* 91 064605.



Prasad, E., K. M. Varier, R. G. Thomas, P. Sugathan, A. Jhingan , N. Madhavan, B. R. S. Babu ,Rohit Sandal ,Sunil Kalkal *et al* ., (2010), Conclusive evidence of quasifission in reactions forming the ^{210}Rn compound nucleus, *Phys Rev C* 81, 054608.

Ramamurthy, V.S., and S.S. Kapoor (1985), Interpretation of fission-fragment angular distributions in heavy-ion fusion reactions *Phys Rev Lett*, Jan 21;54(3):178-181.

Reddy, S., Ramakrishna , A. Pal, S. K., Duggi, T., Santhosh ,Pankaj Shah,Tanya Singh, K. Prameela ,V. V. Parkar, N. N. Deshmukh., *etal.*,(2024), Fission modes in ^{223}Ac and ^{227}Pa compound nuclei, *Phys. Rev. C* 110, 014622.

Shamlath A, M. Shareef, E. Prasad , P. Sugathan , R.G. Thomas , A. Jhingan , S. Appannababu , A.K. Nasirov A.M. Vinodkumar , K.M. Varier , C. Yadav , B.R.S. Babu , S. Nath , G. Mohanto , Ish Mukul , D. Singh, S. S Kailas (2016) , Fission fragment mass distribution studies in $^{30}\text{Si} + ^{180}\text{Hf}$ reaction, *Nuclear Physics A*. 945, January 2016, Pages 67-79.

Sharma Chetan, Bivash Behera , Shruti Narang, Sugathan Pullanhiotan,*et al.*, (2023), Fission dynamics and entrance-channel study in the ^{210}Po compound nucleus via light-particle multiplicities, *Physical Review C* 107(6):064615.

Swiatecki W J., (1981), The Dynamics of Nuclear Coalescence or Reseparation , *Phys. Scr.* 24, 113 DOI 10.1088/0031-8949/24/1B/007.

Tokai.,J., R. Bock, G. X. Dai , A. Gobbi, S. Gralla, K.D. Hildenbrand, J. Kuzminski , W. F.J. Müller, *et al.*, (1985) , Quasi-fission —The mass-drift mode in heavy-ion reactions,*Nuclear Physics A* Volume 4;40, Issue 2, 8 .327-365.

Vikas Kavita, K.S. Golda ,T.K. Ghosh, A . Jhingan *etal* (2024), Reply to “Comment on ‘Fusion-fission dynamics of $\text{Pt}^{188,190}$ through fission fragment mass distribution measurements’ *Phys.Rev.C* 109 , 6, 069802 Published: Jun 20, 2024DOI: 10.1103/PhysRevC.109.069802.

Viola, V. E. , K. Kwiatkowski, and M. Walker (1985) , Systematics of fission fragment total kinetic energy release *Phys Rev C Nucl Phys.* 1985 Apr;31 (4):1550-1552. doi: 10.1103/physrevc.31.1550. 440, Issue 2, , 327-365